Mapping the Limitations of Breakthrough Analysis in Fixed-Bed Adsorption

James Clinton Knox

NASA Marshall Space Flight Center, Huntsville, AL, USA

Introduction: Field of Study

- Gas separation processes using fixed beds of adsorbents are important in many existing and emerging industries
- Adsorbent processes are typically cyclic, with adsorption and desorption steps that swing between high and low pressures, temperatures, or concentrations (PSA, TSA, CSA)
- Computer simulations are typically used to select hardware and process parameters (adsorbent type, layer sizes, pressure and temperature set points, cycle time, flow rate, etc.)
- A cyclic steady-state condition is only reached after many cycles
- Simulation execution speed is critical due to the large trade space and extensive number of cycles required for a single data point

Skarstrom Patent

- Pressure swing adsorption process
- Air drying using silica gel beds
- Cyclic steady state only achieved after 6 days of operation

July 12, 1960 C. W. SKARSTROM 2,944,627
METHOD AND APPARATUS FOR FRACTIONATING GASEOUS MIXTURES BY ADSORPTION
Filed Feb. 12, 1958 9 Sheets-Sheet 2

FIG.-2

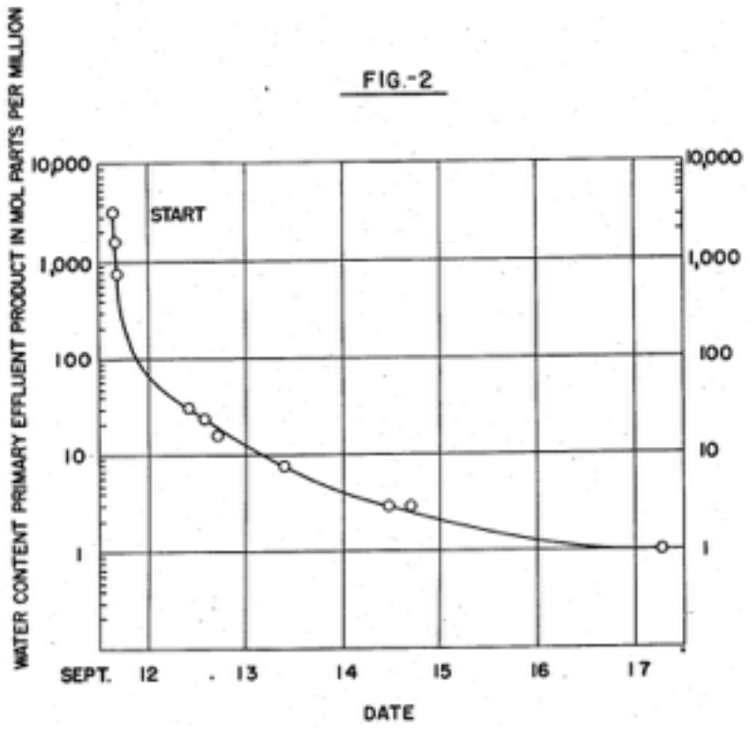

Charles W. Skarstrom Inventor
By A. Abrahamson Attorney

Introduction: Area of Concern

- Execution speed requirements dictate use of simplified one-dimensional model for cyclic process simulations
- 1-D axially dispersed plug flow equation predominantly used in process simulations based on current literature
- Simplifying assumptions include two lumped mass transfer terms requiring empirical determination
- Mass transfer term determination is generally via breakthrough analysis in sub-scale fixed-beds with a low tube diameter to particle diameter ratio

$$\frac{\partial c}{\partial t}+\left(\frac{1-\varepsilon}{\varepsilon}\right)\frac{\partial \bar{q}}{\partial t}-D_L\frac{\partial^2 c}{\partial x^2}=-\frac{\partial v_i c}{\partial x}$$

$$\frac{\partial \bar{q}}{\partial t}=k_n(q^*-\bar{q})$$

Introduction: Research Findings (1)

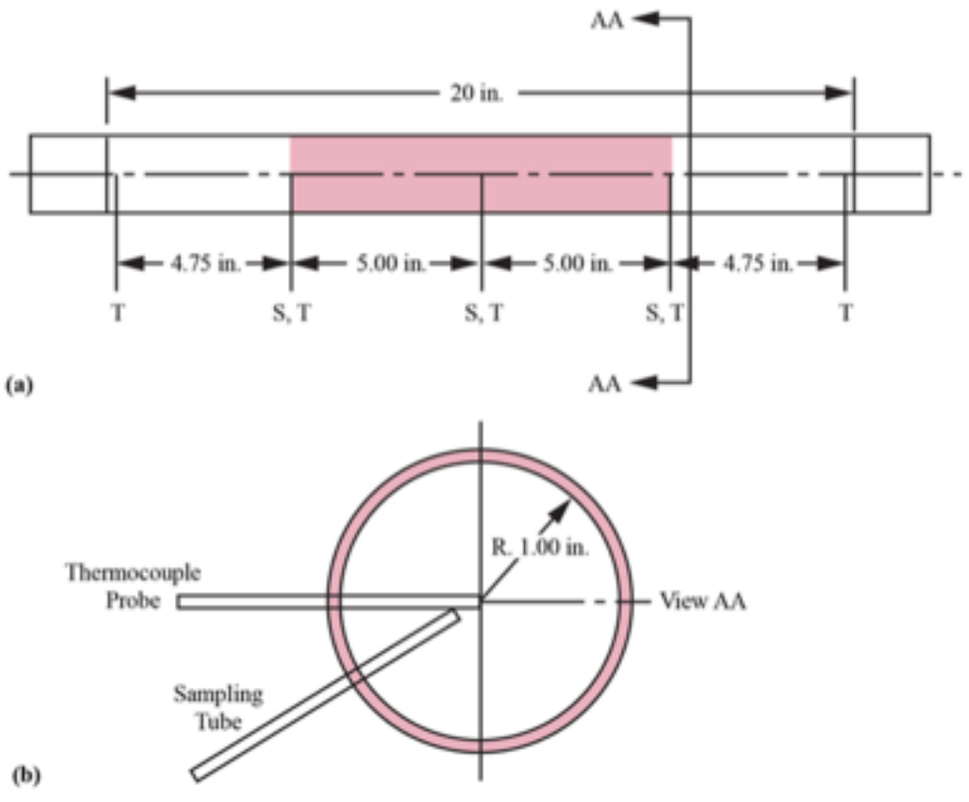

(a) Breakthrough test apparatus and (b) cross-sectional view of a typical temperature measurement and gas sampling location. “T” indicates thermocouple probe location, and “S” indicates sampling tube location. Shading in (a) indicates location of sorbent packing.

Knox, J. C. Finite Difference Modeling and Experimental Investigation of Carbon Dioxide Adsorption on a Molecular Sieve Sorbent Material Used in Spacecraft Carbon Dioxide Removal Systems : A Thesis. University of Alabama, Huntsville, 1992.

- Standard breakthrough analysis is based on measurement taken after mixing of two flow regimes: in the bed core, and channeled flow along the walls
- Resultant inaccuracies in mass transfer term cause errors during simulation-based design of full-scale separation process
- *An improved approach was developed to use a centerline measurement in addition to the mixed measurement and determine terms individually*

Introduction: Research Findings (2)

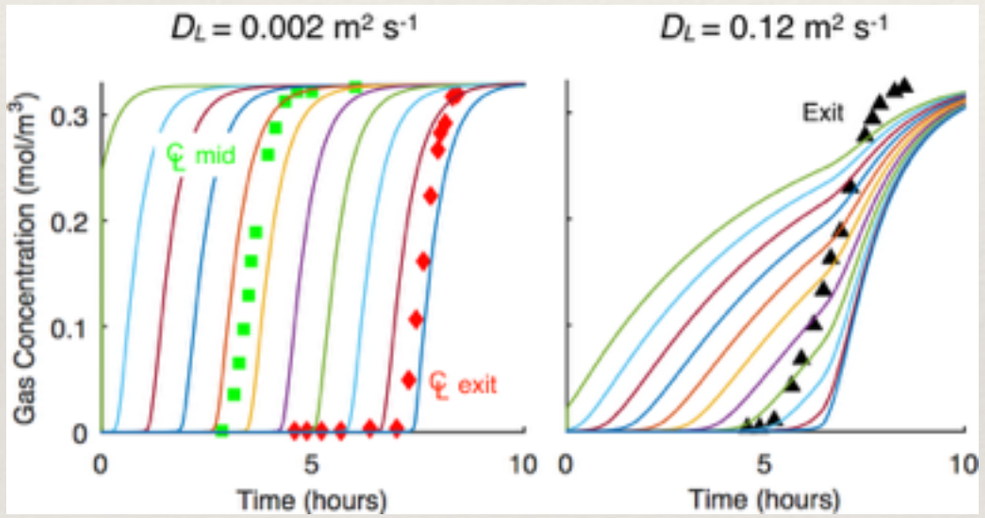

Knox, J. C.; Ebner, A. D.; LeVan, M. D.; Coker, R. F.; Ritter, J. A., Limitations of Breakthrough Curve Analysis in Fixed-Bed Adsorption. *Ind Eng Chem Res* **2016**.

- Axial dispersion term derived based on Fickian (molecular) diffusion, but is used to model dispersion arising from flow around pellets and wall effects
  - *For strongly adsorbed species, interaction of a large dispersion term with the ill-posed Danckwerts boundary condition causes hidden nonphysical simulation result*
- *To prevent nonphysical behavior, limiting expressions for the mass transfer terms were derived for specific sorbent/sorbate pairs and inlet conditions*
- *A generalized expression was derived to limit the mass transfer terms for any sorbent/sorbate pair based on the strength of adsorption*

Principle Equations in 1-D Model

$$\frac{\partial c}{\partial t}+\left(\frac{1-\varepsilon}{\varepsilon}\right)\frac{\partial \bar{q}}{\partial t}-D_L\frac{\partial^2 c}{\partial x^2}=-\frac{\partial v_i c}{\partial x}$$

$$\frac{\partial \bar{q}}{\partial t}=k_n(q^*-\bar{q})$$

$$\varepsilon a_f\rho_f c_{pf}\frac{\partial T_f}{\partial t}-\varepsilon a_f k_{eff}\frac{\partial^2 T_f}{\partial x^2}=-\varepsilon a_f\rho_f v_i c_{pf}\frac{\partial T_f}{\partial x}+a_f a_s h_s\left(T_s-T_f\right)+P_i h_i\left(T_w-T_f\right)$$

$$(1-\varepsilon)\rho_s c_{ps}\frac{\partial T_s}{\partial t}=a_f a_s h_s\left(T_f-T_s\right)-(1-\varepsilon)a_f\lambda\frac{\partial q}{\partial t}$$

$$a_w\rho_w c_{pw}\frac{\partial T_w}{\partial t}-a_w k_w\frac{\partial^2 T_w}{\partial x^2}=p_i h_i\left(T_f-T_w\right)+P_o h_o\left(T_a-T_w\right)$$

$$n=\frac{ap}{\left[1+(bp)^t\right]^{1/t}};\qquad b=b_0\exp(E/T);\qquad a=a_0\exp(E/T);\qquad t=t_0+c/T$$

$$\frac{1}{Pe}=\frac{20}{\varepsilon}\left(\frac{D}{2vR_p}\right)+\frac{1}{2}=\frac{20}{ReSc}+\frac{1}{2}$$

$$\frac{1}{Pe}=\frac{0.73\varepsilon}{ReSc}+\frac{1}{2\left(1+\frac{13\cdot 0.73\varepsilon}{ReSc}\right)}\qquad 0.0377<2R_p<0.607\ \text{cm}$$

$$h_i=\frac{k_f}{2R_i}Nu\quad\text{with}\quad Nu=2.03Re^{0.8}\exp\left(-6\frac{R_p}{R_i}\right)$$

$$c_p=a_o+a_1T_f+a_2T_f^{\,2}+a_3T_f^{\,3}$$

$$Sh=2+1.1Sc^{\frac{1}{3}}Re^{0.6}\qquad h_s=\frac{ShD}{2R_p}$$

$$k_e=k_f\left(\frac{k_s}{k_f}\right)^n\quad\text{with}\quad n=0.280-0.757\log_{10}\varepsilon-0.057\log_{10}\left(\frac{k_s}{k_f}\right)$$

$$k_{eff}=k_f\left(\frac{k_e}{k_f}+0.75PrRe\right)\quad\text{where}\quad Pr=\frac{c_p\mu}{\rho_f k_f}$$

All variables in Mass and Heat Balance Equations are determined except D_L, k_n, *and* h_o

Experimental Results

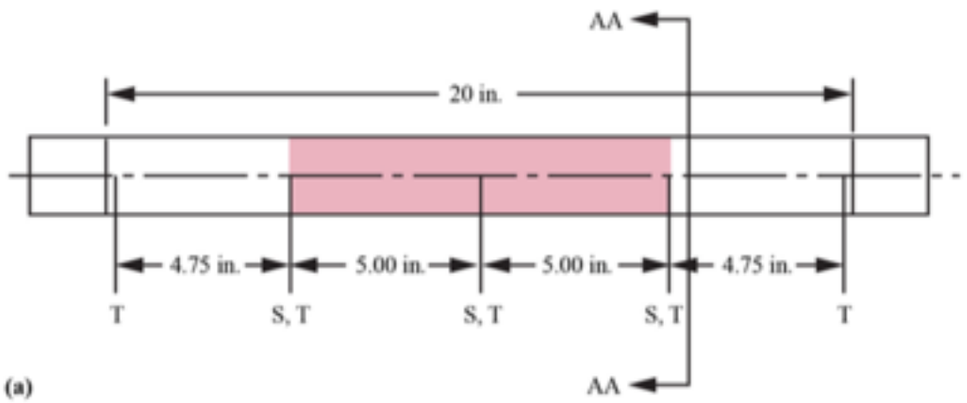

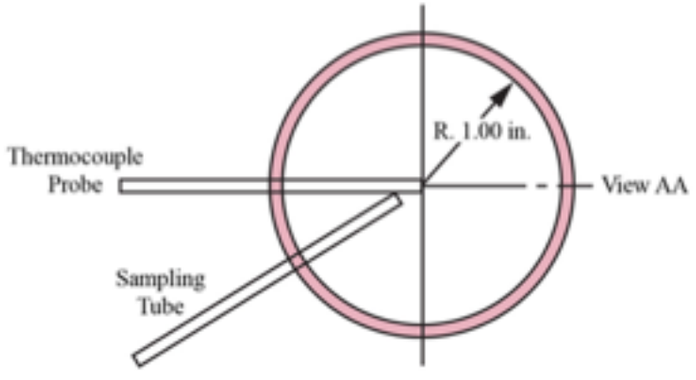

(a) Breakthrough test apparatus and (b) cross-sectional view of a typical temperature measurement and gas sampling location. “T” indicates thermocouple probe location, and “S” indicates sampling tube location. Shading in (a) indicates location of sorbent packing.

Knox, J. C. Finite Difference Modeling and Experimental Investigation of Carbon Dioxide Adsorption on a Molecular Sieve Sorbent Material Used in Spacecraft Carbon Dioxide Removal Systems : A Thesis. University of Alabama, Huntsville, 1992.

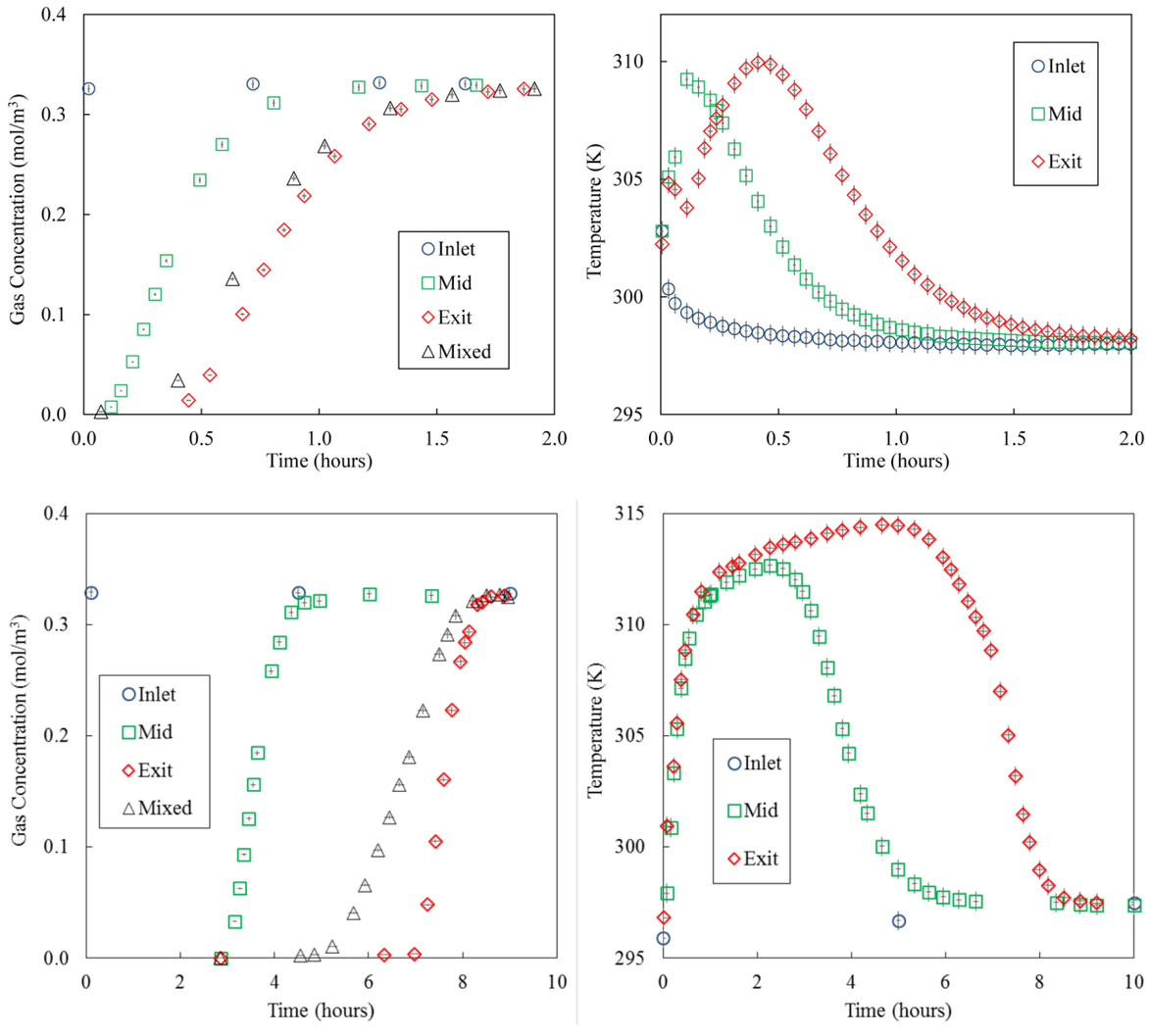

Left panels: Experimental gas-phase concentration profile history breakthrough curves for CO2 (top) and H2O vapor (bottom) on zeolite 5A at 3 centerline locations in the bed (circles: 2.5%, squares: 50%, and diamonds: 97.5%) and just outside the bed (triangles). Right panels: Corresponding experimental temperature profile histories for CO2 (top) and H2O vapor (bottom) on zeolite 5A at 3 centerline locations in the bed (circles: 2%, squares: 50%, and diamonds: 98%). Error bars show experimental uncertainty.

Knox, J. C.; Ebner, A. D.; LeVan, M. D.; Coker, R. F.; Ritter, J. A., Limitations of Breakthrough Curve Analysis in Fixed-Bed Adsorption. *Ind Eng Chem Res* **2016**.

Step 1: Wall to Ambient Heat Transfer Coefficient

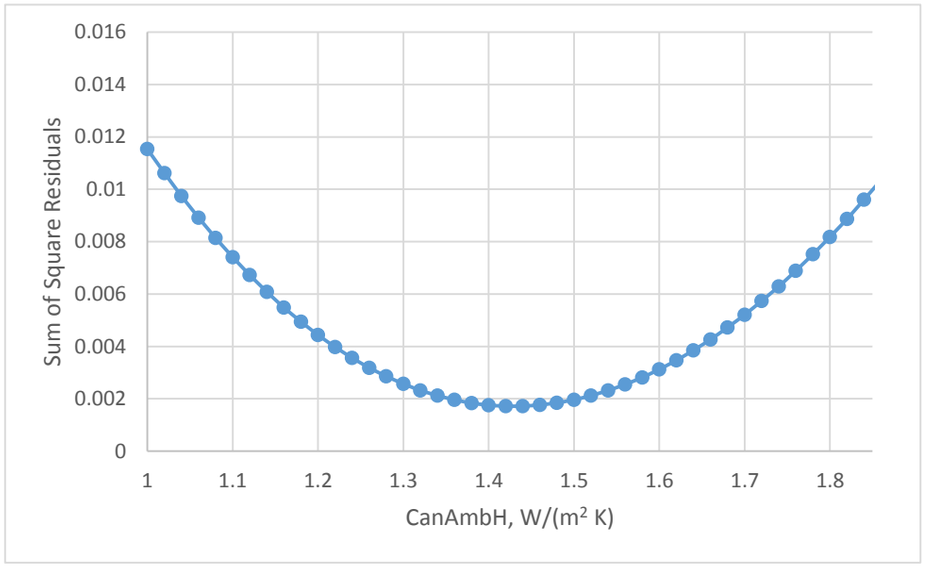

Sum of Square Residuals for Experimental and Simulation Data

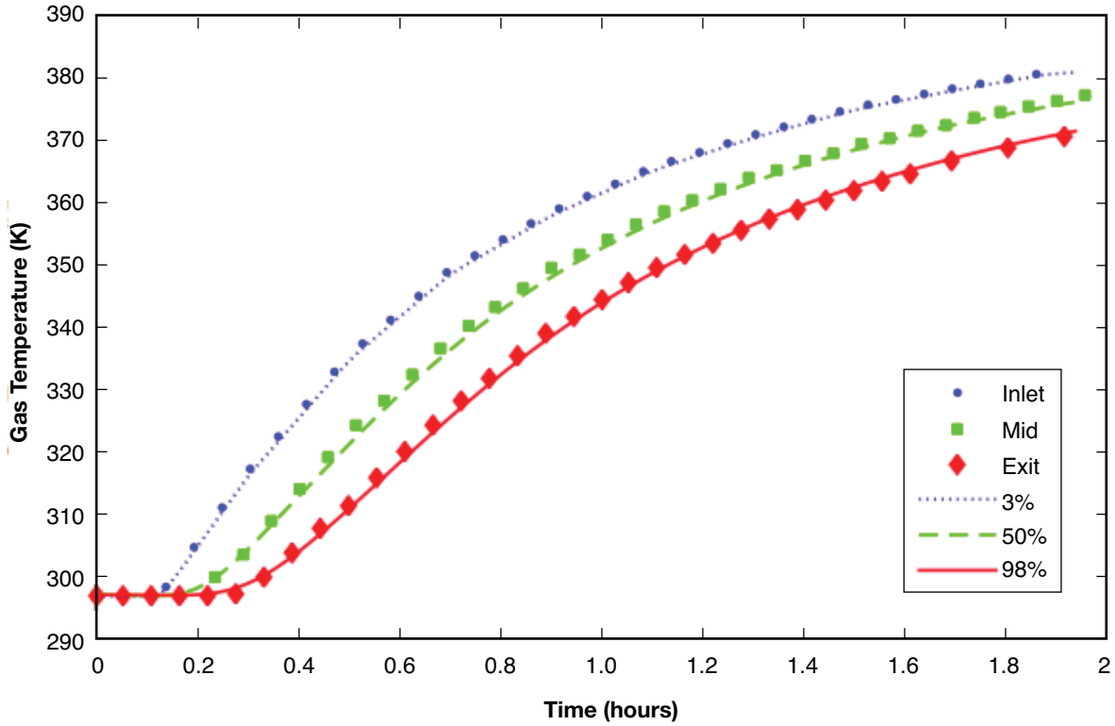

Temperature history data for the thermal characterization test with N_2

h_o is empirically derived via a Thermal Characterization Test

Step 2: Linear Driving Force Mass Transfer Coefficient

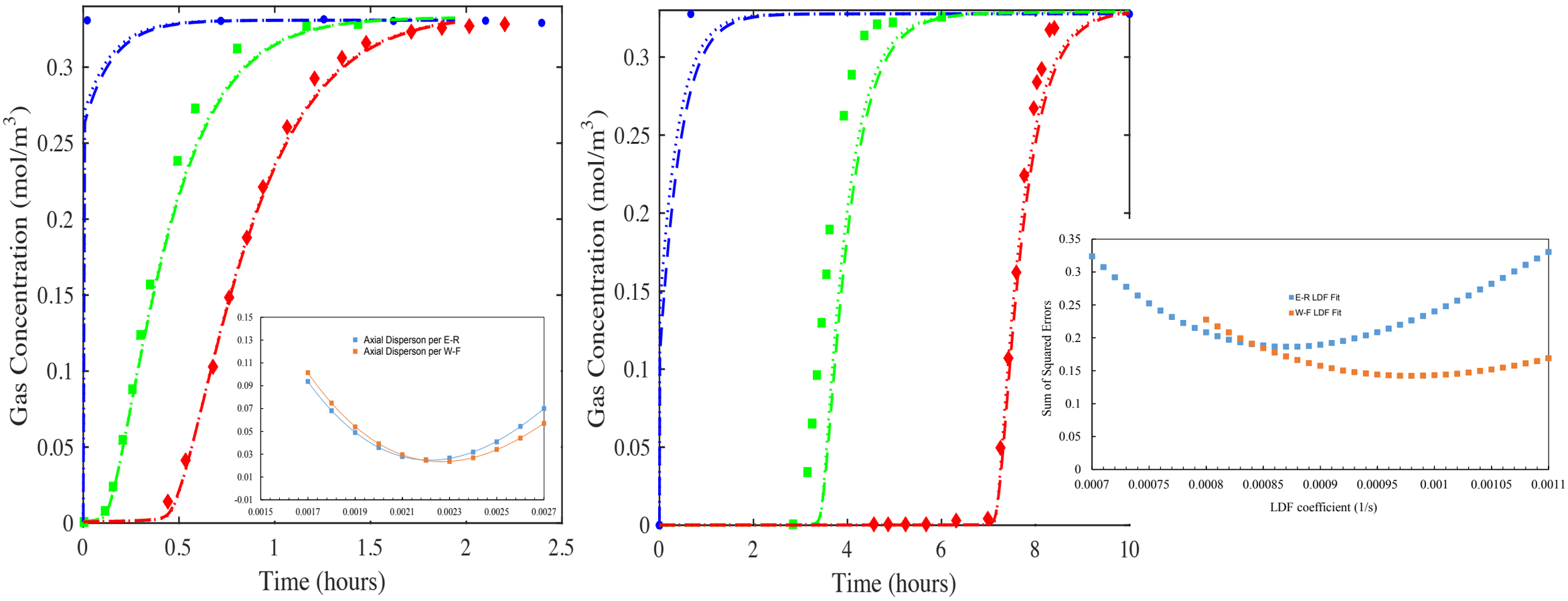

Fits of the 1-D axial dispersed plug flow model to the 97.5% location (diamonds) experimental centerline gas-phase concentration breakthrough curves for CO_2 (left) and H_2O vapor (right) on zeolite 5A, and corresponding predictions from the model of the 2.5% (circles) and 50% (squares) locations. The saturation term in the CO_2-zeolite 5A isotherm was increased by 15%. The saturation term in the H_2O vapor-zeolite 5A isotherm was decreased by 3%. **The void fraction was reduced to 0.33 based on the Cheng distribution (Cheng *et al*., 1991) with C = 1.4 and N = 5, as recommended by Nield and Bejan (1992)**

k_n is empirically derived via fitting to centerline concentration breakthrough curve. For this step, dispersion is taken to result from pellet effects only (no wall effects). Choice of dispersion correlation has a small impact on k_n

Step 3: Axial Dispersion Coefficient (CO_2 Case)

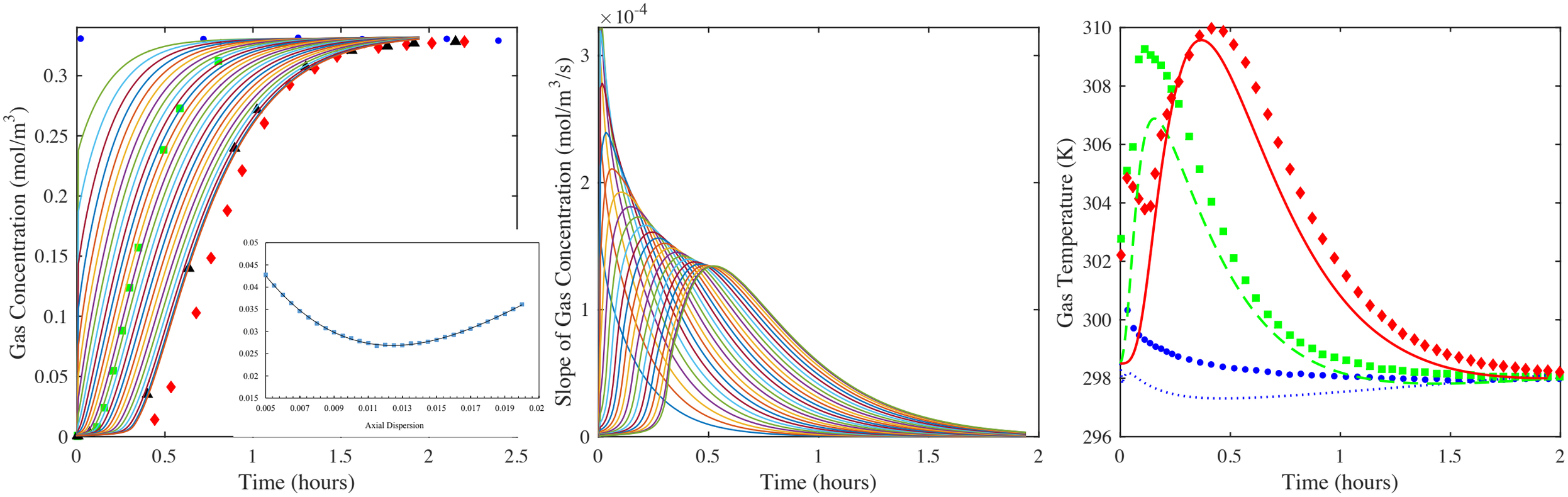

CO_2 on zeolite 5A: Fit of the 1-D axial dispersed plug flow model to the outside bed (triangles) experimental breakthrough curve using a value of D_L 7 times greater than that from the Wakao and Funazkri correlation and the fitted LDF k_n = 0.0023 s^{-1} (left panel). The reported saturation term for the CO_2-zeolite 5A isotherm was used, along with **the reported void fraction of 0.35**. Predictions from the model (lines) of the gas-phase concentration breakthrough curves at 0, 4, 8, 12, …, 92, 96 and 100% locations in the bed are also shown in the left panel, along with the 2.5% (circles), 50% (squares) and 97.5% location (diamonds) experimental center line gas-phase concentration breakthrough curves (left panel). The corresponding derivative (or slope) of the predicted gas-phase concentration breakthrough curves in the bed are shown in the middle panel. Predictions from the model (lines) of the 2.5% (circles), 50% (squares) and 97.5% location (diamonds) experimental center line temperature profile histories are shown in the right panel.

D_L term is fit to mixed gas concentration (far downstream), but requires value 7 times the correlation value to compensate for wall channeling. Fit is specific to the size of the column; for a much larger column wall channeling may be neglected and correlated values of D_L used (but not for fixed beds with a tube to pellet ratio of 20 as in this case, or less)

Step 3: Axial Dispersion Coefficient (H_2O Case)

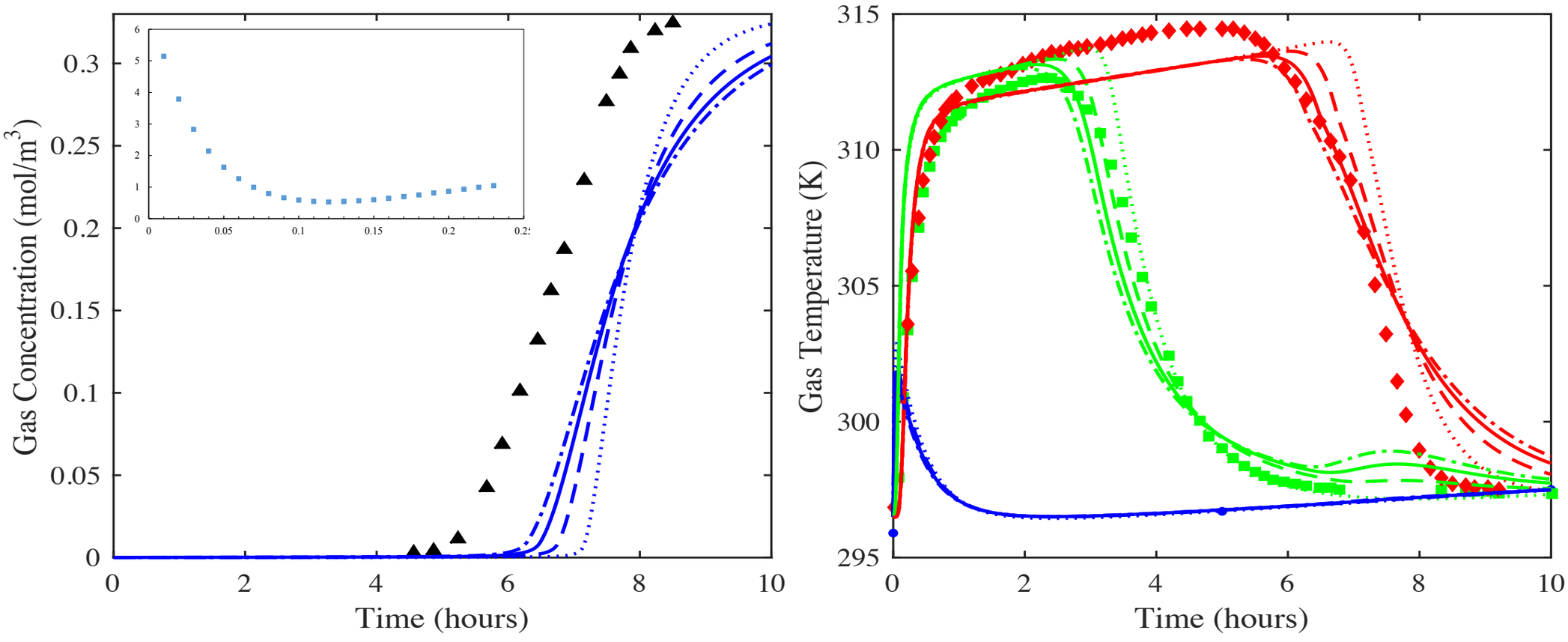

H_2O vapor on zeolite 5A: Predictions from the 1-D axial dispersed plug flow model of the outside the bed (triangles) experimental breakthrough curve when varying the value of D_L. **D_L = 10 (dotted lines), 30 (dashed lines), 50 (solid lines) and 70 (dash-dot lines) times greater than Wakao and Funazkri correlation** with the LDF k_n = 0.00083 s^{-1} (left panel). The reported saturation term for the H_2O-zeolite 5A isotherm was used, along with the reported void fraction of 0.35. The corresponding predictions from the model (lines) of the 2.5% (circles), 50% (squares) and 97.5% location (diamonds) experimental center line temperature profile histories are shown in the right panel.

D_L term is fit to mixed gas concentration (far downstream), but requires value ***50(!)*** times the correlation value to compensate for wall channeling. However the temperature profiles deviate increasingly from the test data with increasing D_L indicating a breakdown of the axial dispersed plug flow model.

Step 3: Axial Dispersion Coefficient (H_2O Case)

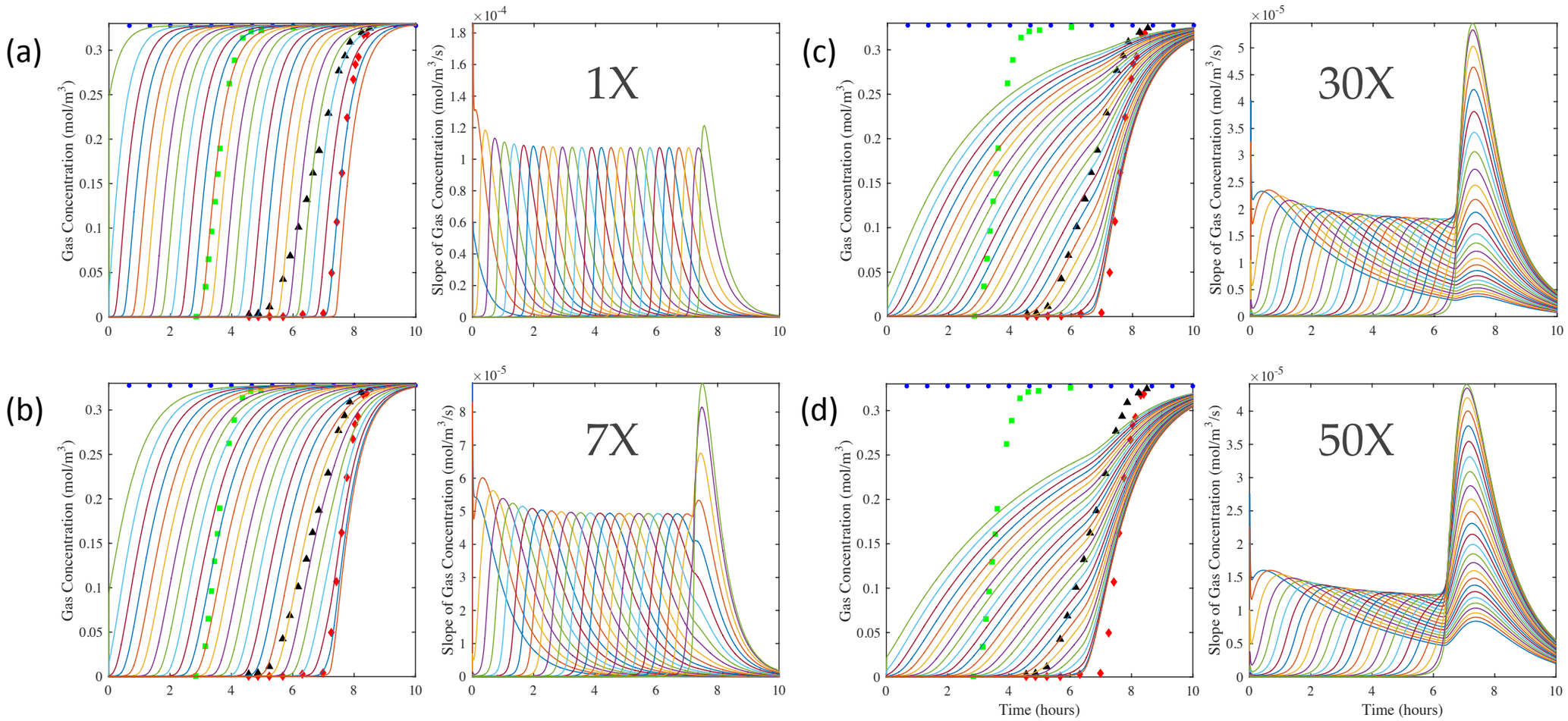

H_2O vapor on zeolite 5A: Predictions from the model (lines) shown in Figure 9 of the gas-phase concentration breakthrough curves at 0, 4, 8, 12, …, 92, 96 and 100% locations in the bed (left panels). The 2.5% (circles), 50% (squares) and 97.5% location (diamonds) experimental centerline gas-phase concentration breakthrough curves are also shown for comparison in the left panels. The corresponding derivatives (or slopes) of the gas-phase concentration breakthrough curves in the bed are shown in the right panels. (a) D_L = Wakao-Funazkri correlation, and (b) D_L = 7, (c) 30 and (d) 50 times greater than Wakao and Funazkri correlation.

At 7X, internal concentration history slope matches mixed concentration just as for CO_2 case. This indicates that same dispersive mechanism occurs regardless of sorbate. To overcome non-physical breakthrough sharpening, D_L must be increased by 50X to decrease breakthrough slope. Expected CPB is lost entirely for this condition.

Modeling Conclusions

- Breakthrough tests with tube diameter to pellet diameter ratios of around 20 (or less), are subject to wall channeling, an mechanism not captured in standard dispersive correlations. Breakthrough tests are generally sub-scale to conserve sorbent materials and gas flow equipment costs and thus frequently in this range.
- The typical breakthrough measurement is taken far downstream, after mixing. Fitting the mass transfer coefficient to this measurement will provide erroneous results for a larger (or smaller) diameter column due to the influence of channeling.
- A method has been demonstrated where a centerline measurement is used to derive a mass transfer coefficient that captures physics free of wall effects and thus appropriate for scale-up to large diameter columns.
- Using the mass transfer coefficient derived above, this method uses the mixed concentration data for fitting of a dispersion coefficient D_L specific to the tube diameter, as needed for processes that utilize small diameter tubes.
- However fitting D_L blindly to the breakthrough curve (as apparent in many published breakthrough analyses) can, in specific cases, result in a complete breakdown of the axially dispersed plug flow model, and result in fitted coefficients that are incorrect.
- Thus it is important to map the set of conditions where significant breakthrough sharpening occurs in order to avoid nonphysical and non-predictive simulation behavior.

Mapping the Sensitivity of Sorbate/Sorbent Systems to D_L and k_n

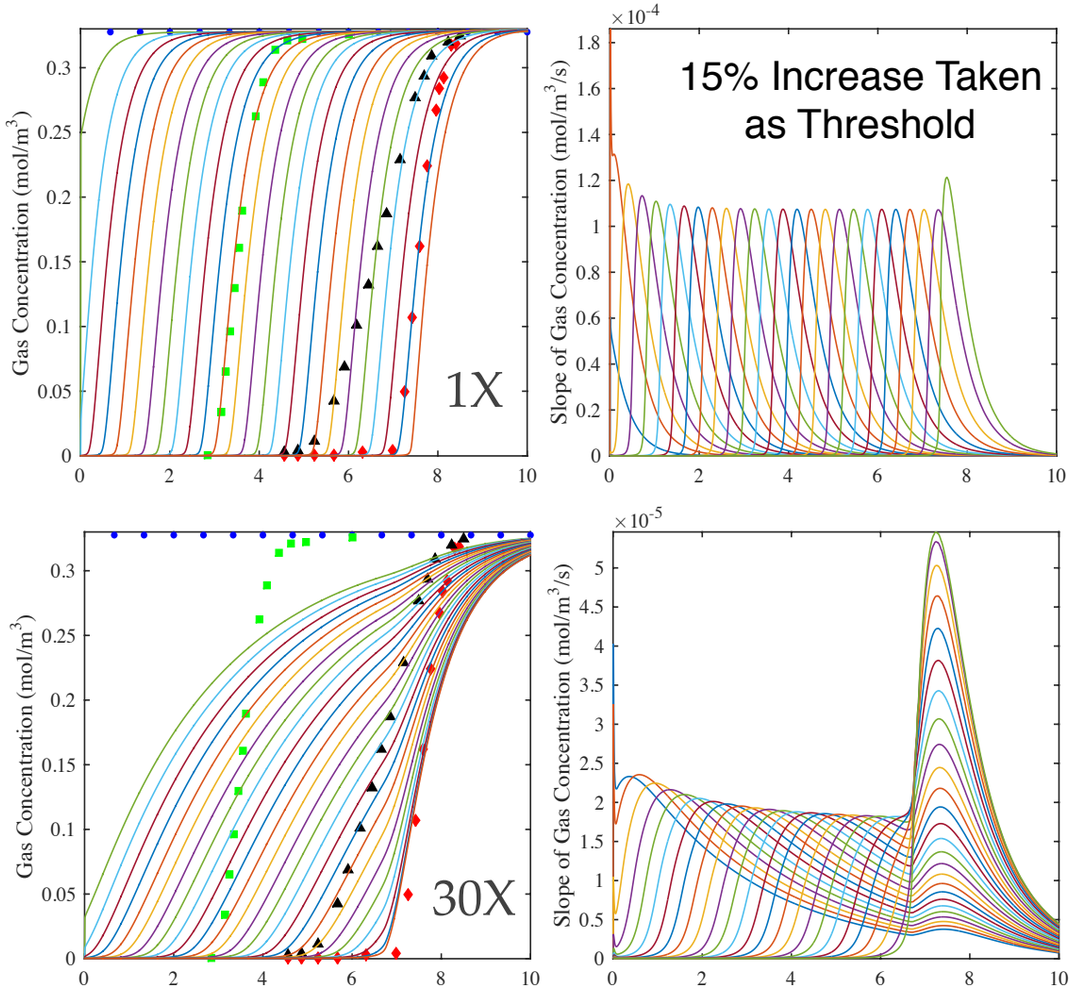

Slope ratio provides metric for breakthrough sharpening and departure from constant pattern behavior

Mass Balance Equations

$$\frac{\partial c}{\partial t}+\left(\frac{1-\varepsilon}{\varepsilon}\right)\frac{\partial \bar{q}}{\partial t}-D_L\frac{\partial^2 c}{\partial x^2}=-\frac{\partial v_i c}{\partial x}$$

$$\frac{\partial \bar{q}}{\partial t}=k_n(q^*-\bar{q})$$

CO_2 and H_2O Capacity Isotherms

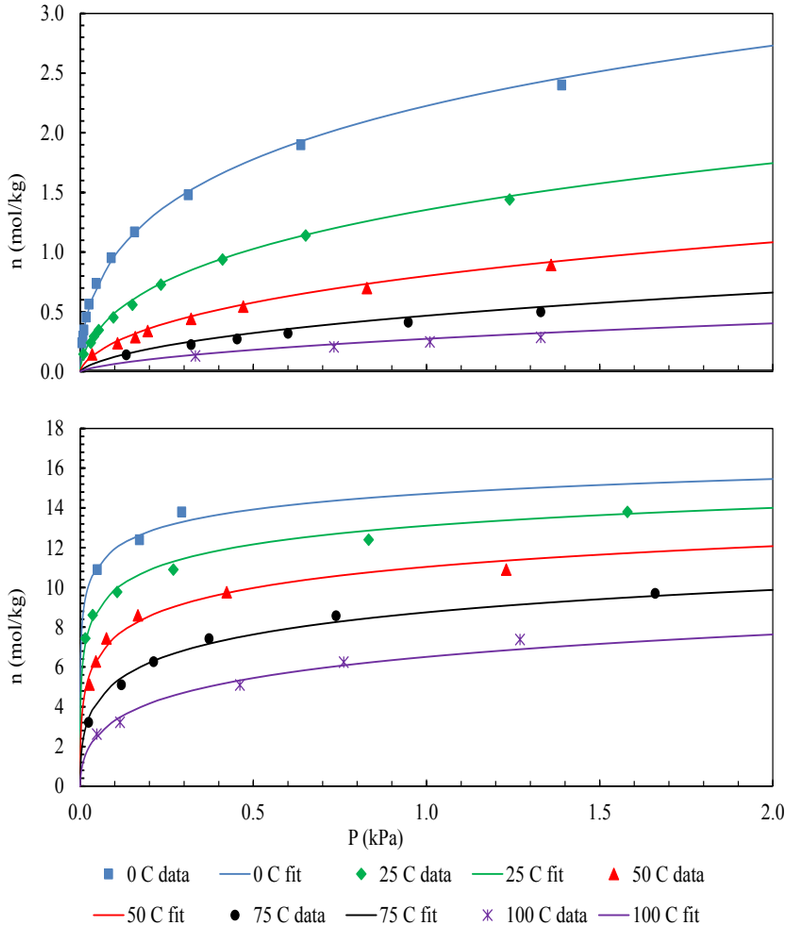

Equilibrium adsorption isotherms for CO2 (top) and H2O vapor (bottom) on zeolite 5A at temperatures from 0°C to 100°C as indicated. Symbols represent experimental data; Toth isotherm fits are shown as lines (Wang and LeVan, 2009)

$$n=\frac{ap}{\left[1+(bp)^t\right]^{1/t}};\qquad b=b_0\exp(E/T);\qquad a=a_0\exp(E/T);\qquad t=t_0+c/T$$

Threshold parameter determination for H_2O on 5A
(similar analysis for CO_2 on 5A, H_2O on 13X, and CO_2 on 13X)

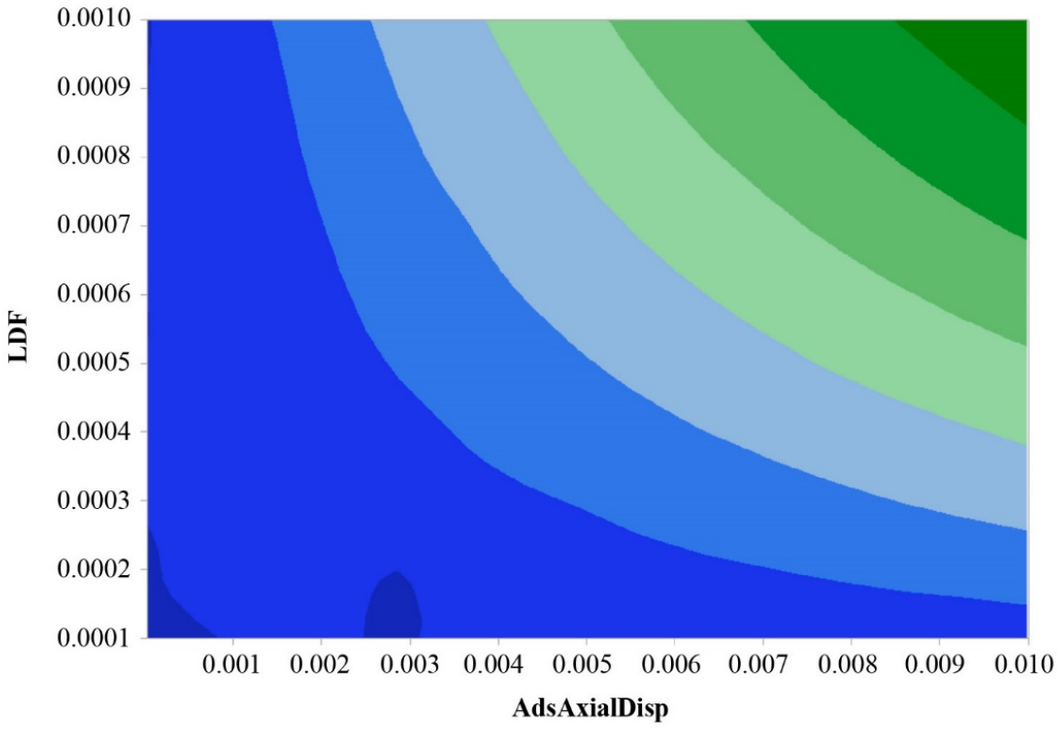

Contour plot of slope ratio for H_2O/5A system based on 100 breakthrough simulations

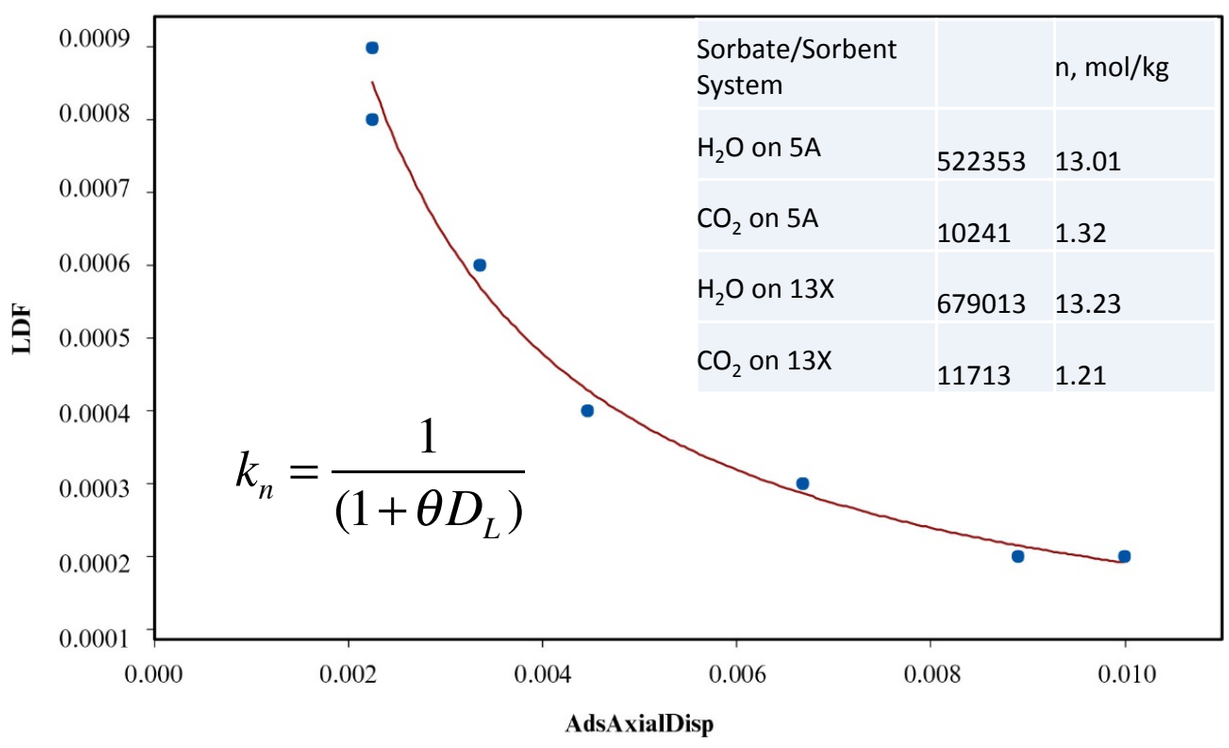

Sorbate/Sorbent System		n, mol/kg
H_2O on 5A	522353	13.01
CO_2 on 5A	10241	1.32
H_2O on 13X	679013	13.23
CO_2 on 13X	11713	1.21

Curve fit of $k_n = f(D_L)$ for simulation runs with slope ratio values between 1.13 and 1.16 for H_2O on 5A. Coefficient of determination (R^2) is 0.998.

For this system, the simulation will result in a slope ratio limit below the threshold if $k_n\left(1+\theta D_L\right)-1<0$

Generalization to any sorbent/sorbate system

$$K_d = \frac{q^*}{q_0^* - q^*}\frac{c_0 - c}{c}$$ Distribution Factor

$$\frac{q^*}{q_m} = \frac{bc}{1+bc}$$ Langmuir Isotherm

$$K_d = 1 + bc_0$$ Distribution Factor for Langmuir Isotherm

Threshold parameter values and distribution factor values

Sorbate/Sorbent System	θ	K_d (fitted)
CO_2 on zeolite 5A	10241	5.213
CO_2 on zeolite 13X	11713	4.862
H_2O on zeolite 5A	522353	33.106
H_2O on zeolite 13X	679013	75.309

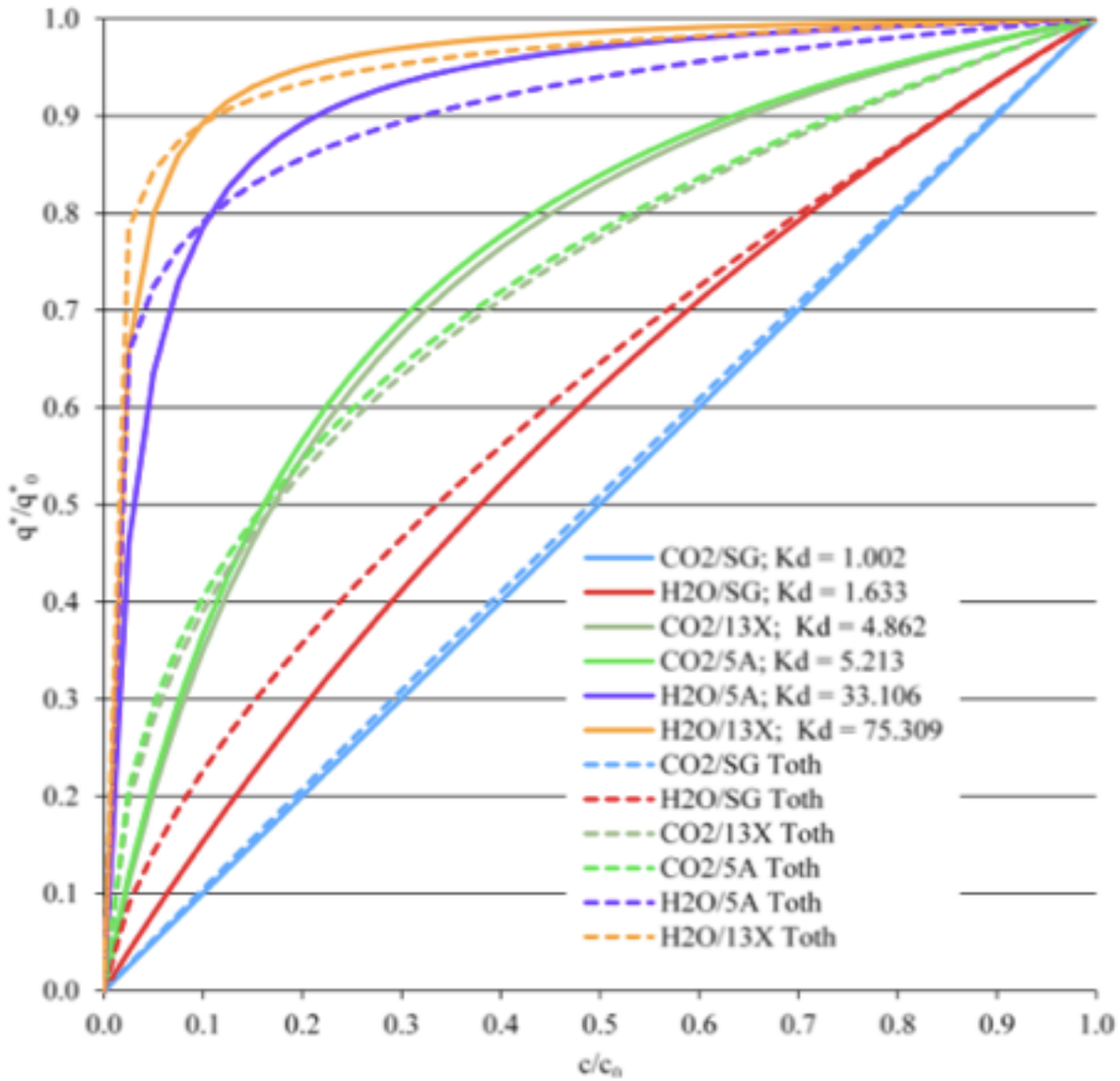

Normalized concentration vs. normalized bed loading for six sorbate/sorbent systems for conditions of 10°C and 1.0 kPa. Solid lines: Langmuir isotherms; Dashed lines: Toth isotherms.

Correlation between threshold parameter and distribution factor

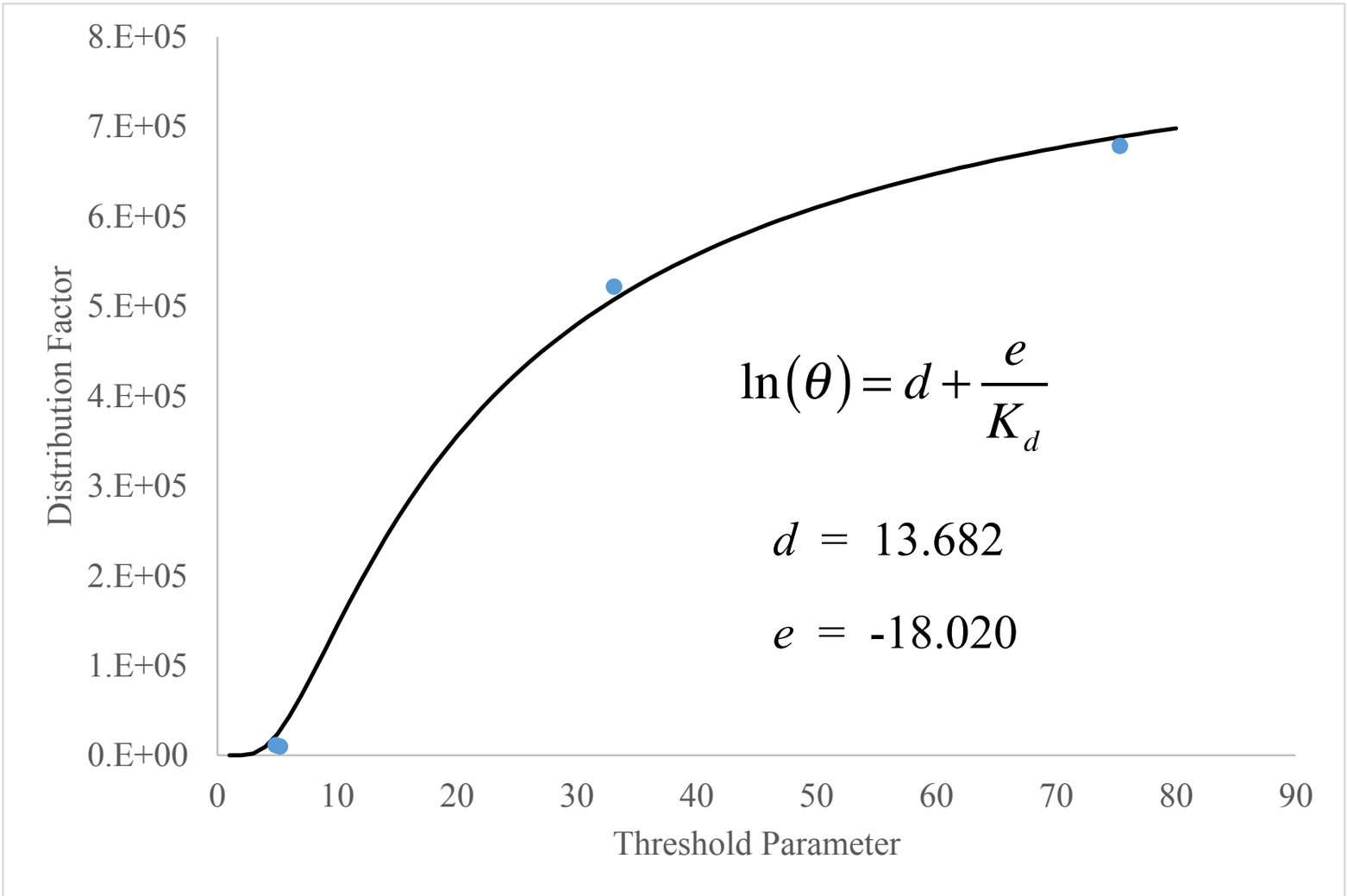

Estimated threshold value q vs. distribution factor Kd for four sorbate/ sorbent systems (filled circles) and fitted relationship shown in Equation 5.6 (line). Coefficient of determination (R^2) is 0.997.

Threshold parameter values and distribution factor values

Sorbate/Sorbent System	θ	K_d (fitted)
CO_2 on zeolite 5A	10241	5.213
CO_2 on zeolite 13X	11713	4.862
H_2O on zeolite 5A	522353	33.106
H_2O on zeolite 13X	679013	75.309

Three-step process to prevent excessive breakthrough sharpening

1. Determine distribution factor (K_d) for sorbent/sorbate system of interest by fitting to Langmuir isotherm

2. Calculate threshold parameter: $$\ln(\theta) = d + \frac{e}{K_d}$$

3. Map limits on D_L vs. k_n plot based on: $$k_n = \frac{1}{(1+\theta D_L)}$$

For values where $k_n(1+\theta D_L)-1<0$ excessive breakthrough sharpening and breakdown of the constant pattern behavior will be avoided

Conclusions for Parameter Mapping

- The axially dispersed plug flow equation and the Danckwerts boundary condition works well for values of dispersion within bounds of accepted correlations
- However, for specific combinations of K_d, D_L and k_n this model breaks down due to the elimination of dispersion at the outlet boundary. In these cases, significant breakthrough sharpening occurs as well as distortion of the internal concentration, deviating from the accepted CPB for these systems.
- This work present a methodology where a threshold parameter may be calculated based on K_d, D_L and k_n, and applied to avoid non-physical model distortion

Overall Conclusions

- The separation of gases through adsorption plays an important role in the chemical processing industry, where the separation step is often the costliest part of a chemical process and thus worthy of careful study and optimization.
- This work developed a number of new, archival aspects on the computer simulations used for the refinement and design of these gas adsorption processes:

1. Presented a new approach to fit the undetermined heat and mass transfer coefficients in the axially dispersed plug flow equation and associated balance equations
2. Examined and described the conditions where non-physical simulation results can arise
3. Presented an approach to determine the limits of the axial dispersion and LDF mass transfer terms above which non-physical simulation results occur

Backup

Gas Separation Processes

- Separation processes are defined as those that transform a mixture of substances into two or more product streams (King, 1980)
- The study of separations is of critical importance as they are the costliest step in many chemical processes, as they reverse the mixing of substances and thus require a decrease in entropy (Yang 2003)

Table 2.1 Common Commercial and Industrial Uses for Sorbents (Keller, 1983; Yang, 2003)

Component to be adsorbed	*Other components*	*Adsorbent(s)*
Gas purification		
H_2O	Olefin-containing cracked gas, natural gas, air, synthesis gas, etc.	Silica, alumina, zeolite (3A)
CO_2	C_2H_4, natural gas, etc.	Zeolite, carbon molecular sieve
Hydrocarbons, halogenated organics, solvents	Vent streams	Activated carbon, silicalite, others
Sulfur compounds	natural gas, hydrogen, liquefied petroleum gas (LPG)	Zeolite, activated alumina
SO_2	Vent streams	Zeolite, activated carbon
Gas bulk separations		
Normal paraffins	iso-paraffins, aromatics	Zeolite
N_2	O_2	Zeolite
O_2	N_2	Carbon molecular sieve
CO	CH_4, CO_2, N_2, Ar, NH_3/H_2	Zeolite, activated carbon
Acetone	Vent streams	Activated Carbon
C_2H_4	Vent streams	Activated Carbon

Table 2.2 Gas Separation and Purification Applications Enabled by New Sorbents (Yang, 2003)

Application	Sorbent and Notes
N_2/CH_4 separation for natural gas upgrading	Clinoptilolite, tinanosilicates by kinetic separation, single-wall carbon nanotubes
CO removal from H2 to < 1 ppm for fuel cell applications	π-complexation sorbents such as CuCl/γ-Al_2O_3, CuY, and, AgY
NO_x removal	Fe-Mn-Ti oxides, Fe-Mn-Zr oxides, Cu-Mn oxides, multi-wall carbon nanotubes
C_3H_6/C_3H_8 (+hydrocarbons) separation	π-complexation sorbents such as CuCl/γ-Al_2O_3, AgNO3/SiO2, AgNO3/clays, aluminophosphate
C_2H_6/C_2H_6 (+hydrocarbons) separation	π-complexation sorbents such as CuCl/γ-Al_2O_3, AgNO3/SiO2, AgNO3/clays

Table 2.3 CO_2 Capture Technologies Funded Under DOE (Vora, 2013).

Project Name	**Project Focus**	**Sorbent Materials**	**Process Approach**	**Technology Maturity**	**Ref.**
Bench-Scale Development & Testing of a Novel Adsorption Process for Post-Combustion CO2 Capture	Novel Adsorption Process	Micro-porous carbon	TSA, fixed-beds	Bench-Scale, Actual Flue Gas	Jain, 2012
Low-Cost Sorbent for Capturing CO2 Emission Generated by Existing Coal-Fired Power Plants	Low-Cost Solid Sorbent	Alkalized Alumina sorbent	Simulated Moving Beds	Bench-Scale Using Actual Flue Gas	Elliot, 2012
CO2 Removal from Flue Gas Using Microporous Metal Organic Frameworks	Micro-porous MOFs	Alumina and Mg/ DOBDC	VPSA	Laboratory-Scale, Simulated Flue Gas	Benin, 2012

Adsorbents and Fixed Beds

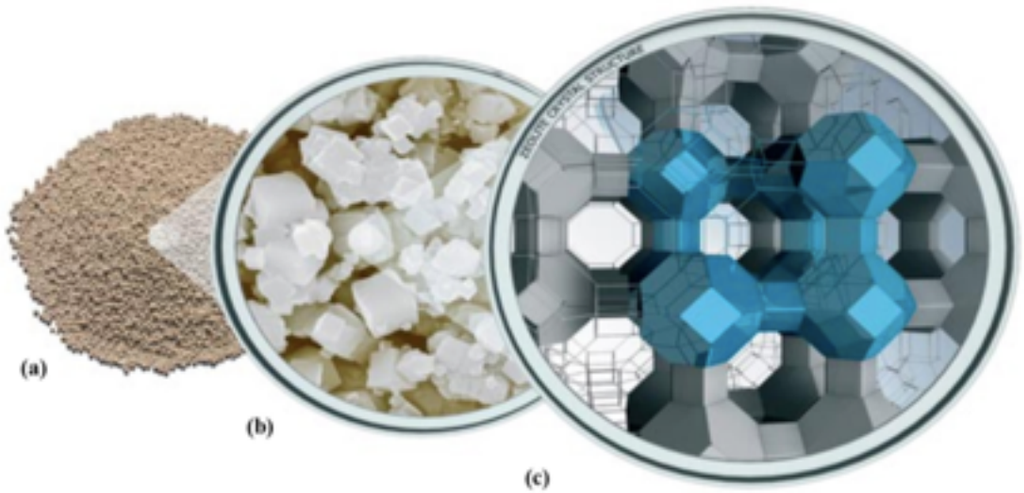

Figure 2.3 (a) Pelletized zeolite pellets, (b) crystals, and (c) framework structure http://www.grace.com/engineeredmaterials/productsandapplications/InsulatingGlass/SieveBeads/Grades.aspx)

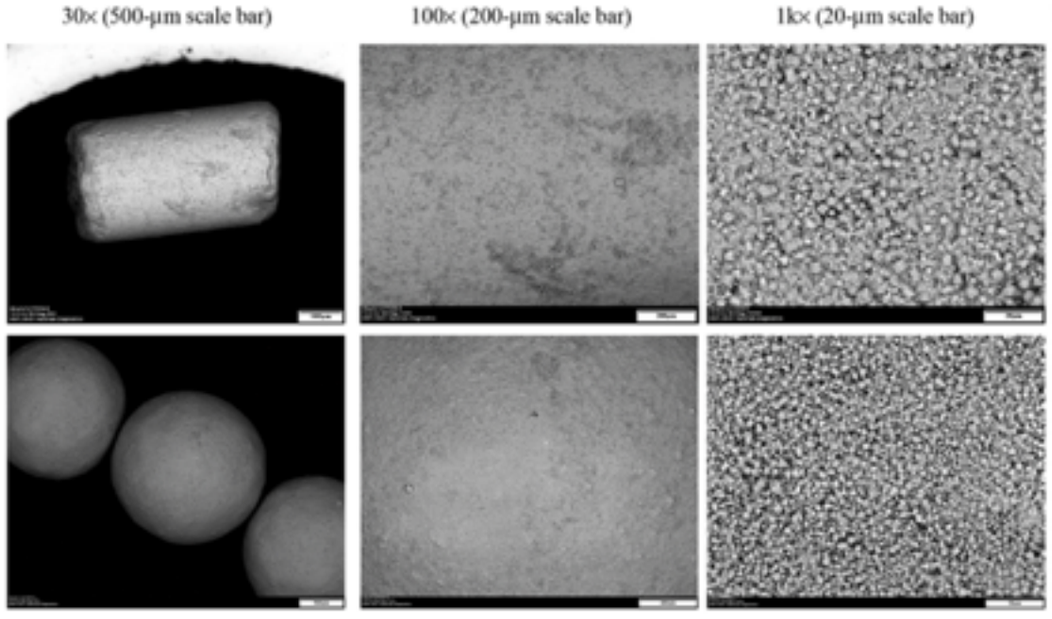

Figure 2.4 SEM images of pelletized zeolite 5A used in the ISS CDRA. Individual zeolite crystals are evident in the 1kx views (Radenburg, 2013).

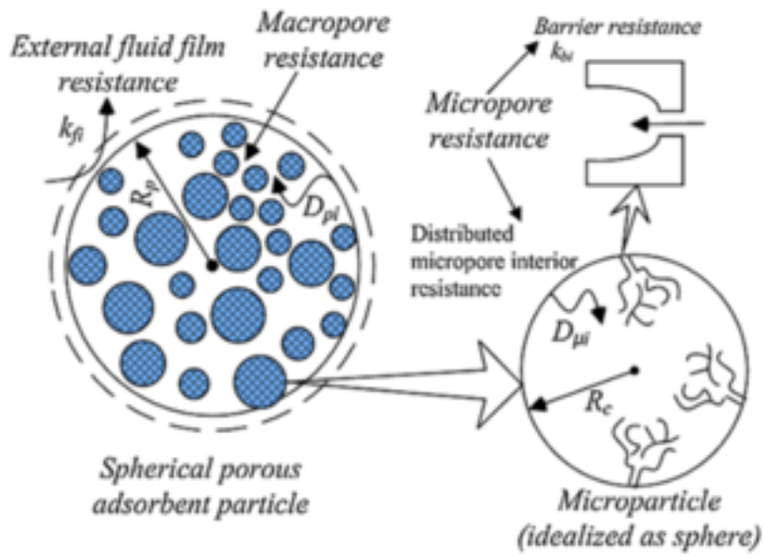

Figure 2.8 Depiction of fixed bed and zeolite mass transfer mechanisms (Shareeyan et al, 2014)

Figure 2.7 Packed (or fixed) bed of zeolite 13X beads. Photo taken by author.

Literature Review of Fixed Bed Gas Adsorption Models

Table A.1 Literature Review of Fixed Bed Gas Adsorption Models

#	Application	Experimental System	Spatial Dimensions	Tube ID/Particle Diameter	Mass Transfer: Gas to Particle Rate Expression	Mass Transfer: Method to Determine Gas to Particle Rate	Axial Dispersion	Internal Profile Shown?	Reference
1	Post-combustion CO_2 capture, steam methane reforming	CO_2 on hydrotalsite (dry and wet)	1	14	Modified LDF: function of loading and isotherm (pore diffusion model)	Breakthrough analysis (adsorb and desorb)	Estimated per Edwards and Richardson 1968	no	Ding and Alpay 2000
2	Hydrogen purification	H2, CO_2, CH4, CO on 5A, Activated Carbon	1	8 and 15	LDF	Breakthrough analysis (Park et al. 1998)	none	no	Park et al., 2000
3	CO_2 scrubbing	H_2O and CO_2 on 5A	1	20	LDF	Breakthrough analysis	Estimated per Edwards and Richardson 1968	yes	Mohamadinejad et al., 2000
4	Dehumidification of organic solvents	H_2O and Acetone on 4A	2	40	Bi-disperse pellet modeled	Not specified	Breakthrough Analysis	no	Penichev and Seikova, 2002
5	Dehumidification of organic solvents	H2O on Silica gel, 13X	1	10	LDF	Uptake curve analysis (Yang and Lee, 1998)	Estimated per Wakao and Funazkri, 1978	no	Ahn and Lee, 2003
6	CO_2 scrubbing	CO_2 and H_2O on 5A	2	20	LDF	Breakthrough analysis	Estimated per Edwards and Richardson 1968	Yes (CO_2 only)	Mohamadinejad et al., 2003
7	Drying of instrument air	H_2O on 4A	1	10	Modified LDF as a function of pressure, temperature and molar fraction	Breakthrough analysis	none	no	Gorbach et al., 2004
8	Dehumidification of organic solvents	H2O on Silica gel, Alumina, 13X	1	10	LDF	Breakthrough analysis (Ahn and Lee, 2003)	Estimated per Wakao and Funazkri, 1978	no	Ahn and Lee, 2004
9	Oxygen purity	O2, Ar, and N2 on CMS	1	n/a	Modified LDF (concentration-dependent diffusivity combined with	Estimated per Bae and Lee (2005)	yes	no	Jee et al., 2005
10	Post-combustion CO_2 capture	CO_2 and N2 on silicalite	1	11	LDF	Estimated per Farooq and Ruthven 1990	Estimated per Wakao et al., 1978	no	Delgado et al., 2006
11	Gas Separation	CH4 and CO_2 on 5A, butane and pentane on silicalite	1	8	Double LDF	Estimated per method reported in this paper, adjusted via breakthrough analysis	Included but not defined	no	Leinekugel-le-Cocq et al., 2007
12	Hydrogen purification	CO on 5A (4 samples) and AC in H2	1	7 and 11	LDF	Breakthrough analysis	Estimated per Lopes et al., 2009	no	Bastos-Neto et al., 2011
13	Post-combustion CO_2 capture	CO_2 and N2 on 13X	1	6	Combined LDF and QDF	Breakthrough analysis	None	No	Won et al., 2012
14	Capture of hydrocarbon emissions from gasoline engines during the cold start period of the engine	Propane on Na-ZSM-5	1	256	LDF	Estimated from film and micropore calculations per Brosillon et al. 2001	Yes (not specified)	Yes	Puertolas et al., 2012
15	Post-combustion CO_2 capture	CO_2 on 13X	1	21	Macropore and micropore solved simultaneously	Estimated + breakthrough analysis	Estimated per Wakao and Funazkri, 1978	Yes	Mulgundmath et al., 2012
16	Post-combustion CO_2 capture	CO_2 and N2 on carbon	1	9, 3	LDF	Breakthrough analysis and estimated via Ruthven 1984	None	No	Gonzlez et a., 2013
17	Development process of a reactor design for open thermochemical energy storage	H_2O on 13X	2	25	LDF	Breakthrough analysis	Yes	Temperature only	Mette et al., 2014
18	Drying of ethanol for fuel production	Ethanol and H_2O on 3A	1	6	LDF	Breakthrough analysis	None	Yes	Kupiec et al., 2014
19	Dehumidification of gases containing organic component	H_2O and benzene on Silica gel, 13X, activated carbon	1	n/a	LDF	Breakthrough analysis (Ko et al., 2002, Park and Knaebel 1992, and Ahn and Lee 2003)	Estimated per Edwards and Richardson 1968	No	Nastaj and Ambrozek, 2015

- Criteria for inclusion:
  - Published in 2000 or later
  - Includes description of experimental data used for validation
- 1-D model used in 16 publications
- Tube to particle diameter ratio ≤ 20 for 16 (most much lower)
- LDF used in 12 publications
- Axial dispersion used in 14 publications
- Breakthrough curve only shown in 14 publications